Advances in Technology Innovation, vol. 8, no. 4, 2023, pp. 278-289

Humidity Control for Air Circulation in the Drying Process

Aphisik Pakdeekaew[1], Krawee Treeamnuk[1,*], Tawarat Treeamnuk[2]

[1]School of Mechanical Engineering, Suranaree University of Technology, Nakhon Ratchasima, Thailand

[2]School of Agricultural Engineering, Suranaree University of Technology, Nakhon Ratchasima, Thailand

Received 20 April 2023; received in revised form 19 July 2023; accepted 20 July 2023

DOI: https://doi.org/10.46604/aiti.2023.12030

Abstract

Recycling exhaust air is acknowledged as a method to reduce the energy consumption of agricultural products in the dryer. This study investigates the performance of an air circulation system at a laboratory scale and develops a feedback control compensator for optimizing the drying air circulation process. A servo motor is employed to drive a valve, to feed the exhaust drying air with high temperature and humidity back in different proportions. The system is controlled using an Arduino DUE microcontroller, which communicates data with MATLAB/Simulink. The system identification methodology is employed to analyze the mathematical model of the system. The result indicates that the response of the system meets the acceptance criteria when the percent overshoot is less than 25%, and the settling time is within 60 seconds (with a 2% error tolerance). Evaluation of control system performance during equilibrium employs R2 and RMSE values.

Keywords: air humidity ratio, drying, humidity control, system identification

1. Introduction

Agricultural products, especially cereal grains like rice, wheat, corn, and beans, are crucial for survival because of their high nutritional content and ability to be processed into a wide range of cuisines [1-2]. Drying is one of the important postharvest steps that is used to reduce the moisture content of the postharvest to an appropriate level. This practice helps to avoid the issue of excessive humidity in the product, which leads to the growth of microorganisms and degradation in the quality of the food during storage [3-4].

In general, to dehumidify agricultural materials and food, solar drying is preferred, which uses less energy costs to reduce moisture because it uses natural heat as an energy source to expel moisture from agricultural materials. However, inclement weather limits this method, and it is vulnerable to animals and insects. Furthermore, it needs a certain amount of manpower and instruments to handle, which raises the production cost. Due to the limits of traditional solar drying techniques, mechanical dryers that can operate in all seasons and control the quality of crops are increasingly popular in the grains production industry [5]. Mechanical dryers are developed from different techniques depending on the purpose of drying and the value of the product [6-7].

When talking about drying paddy, it is the main export product of Thailand's hot air dryers. As for Thailand hot dryers, owing to their simplicity and suitability for practical operations, they are mostly used as a medium in the mechanical dryer to remove moisture from materials. From the review of past research, it was found that the Louisiana State University (LSU) dryers were popular in the paddy industry with energy consumption in the range of 3.874-6.25 MJ/kg water [8-9], while

* Corresponding author. E-mail address: krawee@sut.ac.th

English language proofreader: Chih-Wei Chang

crossflow dryers had energy consumption in the range of 1.94-3.89 MJ/kg water [10-11], and rotary dryers have energy consumption in the range of 2.64-9.2 MJ/kg water [12-13]. These dryers require a high amount of energy to drive the system, which is the energy cost that affects production costs the most.

According to Thailand's 20-year energy conservation plan (2011-2030), the importance of reducing greenhouse gas emissions has been considered, which is the crucial factor that causes the national energy system to transform into a carbon reduction system [14]. As a result, the use of electricity to produce hot air for drying is an advantage compared to using combustion as a heat source. An important method that can reduce energy consumption in the drying process with a hot air dryer is to recirculate the air that has taken moisture from those agricultural materials to be used in the dryer again.

Recently, Amantéa et al. [15] applied reheated air circulation to grain drying. It was found that air recirculation can increase moisture extraction rate, exergy, and energy efficiencies by 25% or more. Sila et al. [16] reported that higher air circulation ratios resulted in lower energy consumption in the air preheating system. These studies have yielded results in the same direction as Darvishi et al. [17], who studied the effect of air circulation on energy consumption during fluidized bed drying of sliced mushrooms under various drying conditions. They found that recycling the exhaust air greatly reduced energy consumption.

Although exhaust air recirculation is an interesting approach to improving the hot air-drying process and has great potential to reduce energy consumption, grains are naturally biomaterial and susceptible to rapid changes in temperature and humidity in the air, especially in dryers. It directly affects the quality of the product [18-19]. Therefore, exhaust air recirculation is necessary to precisely control the air mixing to achieve the desired proportion of air humidity ratio before entering the drying process. The previous research conducted by Pakdeekaew et al. [20] highlighted limitations in the operation of the solenoid valve utilized in the air humidity control system. These limitations pertain to the long-term performance of the equipment and its limited capacity to recycle air, not exceeding 15.18% of the total air volume used in the drying system. Overcoming these challenges presents a significant obstacle in implementing this system effectively within a commercial dryer.

The objective of this study was to design an air humidity control system for grain drying systems, while addressing the limitations identified in previous research. The main focus was on developing a controller that could effectively regulate the humidity ratio of mixed air, comprising recirculating air and ambient air. To achieve this, a butterfly valve was employed to precisely adjust the flow of recycled drying air. The expected outcome of implementing this control system in a commercial hot air dryer is to enhance energy efficiency and ensure better product quality control after the drying process, thus offering promising prospects for the future.

2. Materials and Methods

A drying demonstration set was developed to investigate the design of the humidity control system. The main components comprise a heater and a nozzle spray unit to simulate the transfer of moisture from the drying material to the air in the drying system.

2.1. The drying system on a laboratory scale

The drying demonstration set was used to imitate the circumstances of heat and mass transfer instead of a real drying system. The transfer of moisture from material to air was studied, and the control system of air humidity ratio at point 3 (Fig. 1, mixed air) was developed. The ambient air entering the system (Fig. 1, point 1: Ambient air) and humid air after receiving the moisture from the spray chamber are to be mixed in different proportions (Fig. 1, point 2: Recirculating air). The components of the drying demonstration set are shown in Fig. 1. In Fig. 1, the air was circulated by a 24V 5.5A DC electric blower in this test. Ambient air entered the system at point 1 and flowed through point 3 to the venturi flow meter. At this

point, the air velocity was maintained at 6 m/s (The volumetric flow rate is 0.01478 m^3/s) throughout the test with a regulated DC power supply (ATTEN model APR3010H). Before entering the water spray chamber, the air was heated by the heater that collaborates with a proportional-integral-derivative (PID) temperature controller (RKG model REX -C100FK02) to maintain a consistent air temperature of 70 ˚C.

In the water spray chamber, the spray nozzles simulate the humidification of the air, similar to the process in a drying room where the moisture from the material is transferred to the air. The pressure for the spraying system was provided by a high-pressure pump (SEAFLO model SFDP1-013-100-22, 12 V 5 A, pressure 100 PSI) to spray water in the chamber. A heat and mass transfer process happeneds when hot air collidedes with water mist. As a result, the relative humidity of air rose while the air temperature fell [21]. The humidity ratio of air after the mixing process at point 3 was assessed by the dry bulb temperature and relative humidity of the air. The DHT22 sensor (AM2302 modules, accuracy: humidity ±2% RH (Max ±5% RH); temperature < ±0.5 ˚C; operating range: humidity 0-100% RH; temperature -40-80 ˚C) was utilized to measure it.

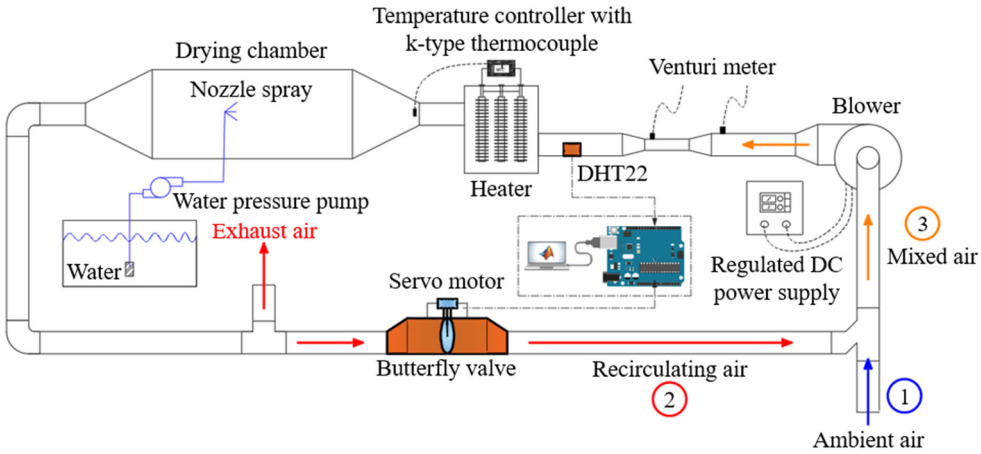

Fig. 1 Schematic diagram of the drying demonstration set

This research used an Arduino DUE as a microcontroller to control the operation of the air circulation system, with a servo motor driving the butterfly valve to adjust the return air ratio as shown in Fig. 2. The percentage of valve opening from 0-100% was defined as the input signal to the system, and its response was the humidity ratio of the air obtained from the mix of recirculating air and ambient air.

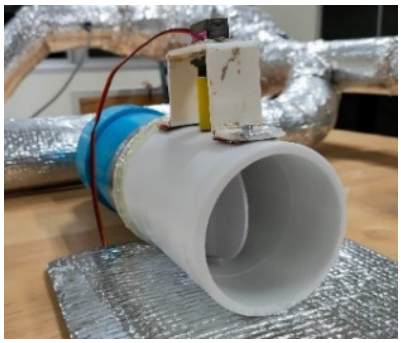

Fig. 2 An adjustable airflow valve

2.2. *The humidity ratio calculation*

This research was focused on controlling the humidity ratio as the response variable (output signal). Calculation of the humidity ratio starts with the DHT22 sensor sensing the dry-bulb temperature of the air in degrees Celsius (˚C) and converting to Kelvin (K) before computing the saturation vapor pressure of air by:

$$P_{sv} = e^{C_1/T_{db}+C_2+C_3T_{db}+C_4T_{db}^3+C_6 lnT_{db}} \quad (1)$$

while the relative humidity of air was used for calculating the vapor pressure

$$P_v = \frac{RH \times P_{sv}}{100} \tag{2}$$

after that, the vapor pressure of air was utilized to calculate the air humidity ratio [22].

$$\omega = 0.621945 \times \frac{P_v}{101325 - P_v} \tag{3}$$

where P_{sv} is the saturation vapor pressure of air (Pa), P_v is the vapor pressure of air (Pa), T_{db} is the dry-bulb temperature of the air (K), RH is the relative humidity of air (%), C_1 is -5.8002206E+03, C_2 is 1.3914993E+00, C_3 is -4.8640239E-02, C_4 is 4.1764768E-05, C_5 is -1.4452093E-08, C_6 is 6.5459673E+00, and ω is the humidity ratio of air.

2.3. Mathematical model of the humidity control system from drying air recirculation

The operation of the humidity control system, which utilized circulating drying air, is shown in Fig. 3. Before entering the air mixing point, the drying air flow rate was proportioned by a butterfly valve driven by a DC servo motor. The recirculated drying air was mixed with the ambient air entering the dryer according to the adiabatic mixing of two air streams process at the mixing point. The percentage of valve opening was defined as the input signal. The air humidity ratio after the mixing process was defined as the output signal. Fig. 4 shows the overall operation block diagram of the system, consisting of 3 main parts as follows: (1) Motor position control system ($G_{position}$), (2) Transfer function between recirculating drying air flow rate and valve angular distance (G_{valve}), and (3) Transfer function of air mixing point ($G_{mixing\ point}$). Each section was combined into a system transfer function model (G_{total}) used for system identification in Section 2.4.

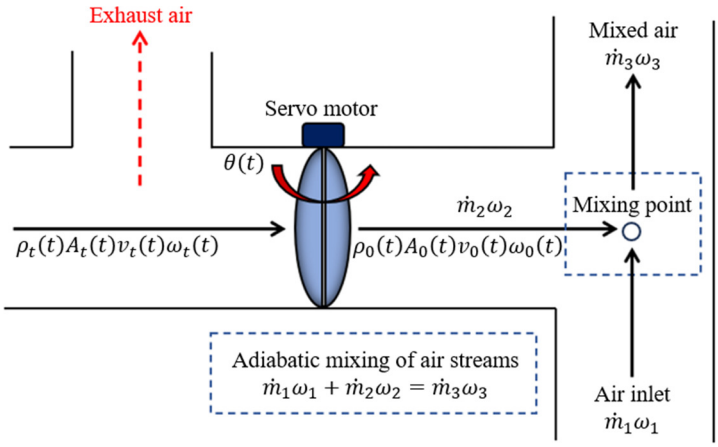

Fig. 3 Functional diagram of the air recirculation proportional control valve

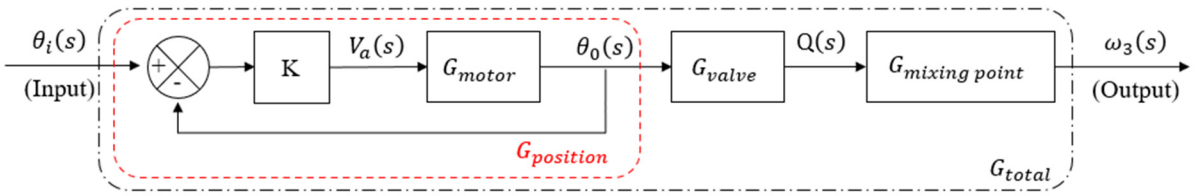

Fig. 4 Block diagram of a humidity control system from recirculating drying air

Aloo et al. [23] reported that the operation of DC motors can be controlled by adjusting the voltage applied to the armature circuit, also known as armature control. Newton's law and Kirchhoff's voltage law were used to analyze this electromechanical system. The transfer function of the motor is shown as:

$$G_{motor}(s) = \frac{\Omega_m(s)}{V_a(s)} = \frac{K_t}{(L_a s + R_a)(Js + f_v) + K_t K_b} \tag{4}$$

Electrical time constants are neglected consideration since they are very small compared to mechanical time constants. Therefore, Eq. 4 can be reduced [24].

$$G_{motor}(s)=\frac{\Omega_m(s)}{V_a(s)}=\frac{K_t}{R_a(Js+f_v)+K_tK_b} \tag{5}$$

The analysis of the angular position of the servo motor can be derived by multiplying the rotational angular velocity with the integrator, as illustrated in Fig. 5.

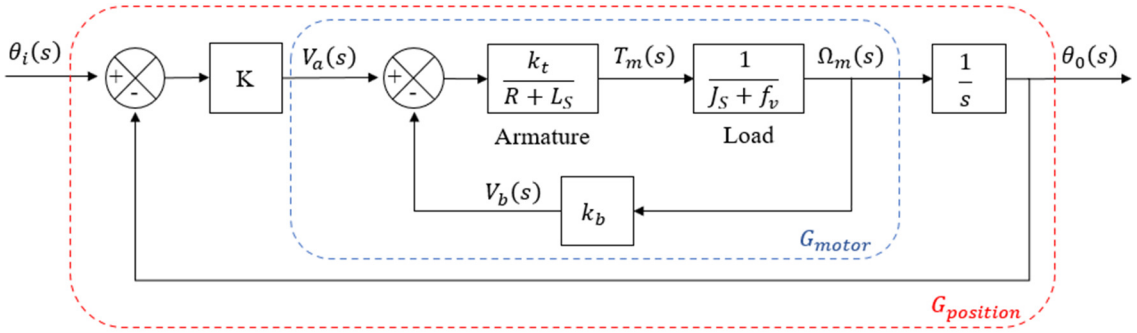

Fig. 5 DC motor position control block diagram

Consequently, the transfer function of the servo motor position control system can be expressed as,

$$G_{position}(s)=\frac{\theta_o(s)}{\theta_i(s)}=\frac{K_TK}{\tau s^2+s+K_T} \tag{6}$$

which describes the relationship between the angular position output and input signals. Where Ω_m is the angular velocity of the motor (rad/s), V_a is the applied armature voltage (V), K_t is the motor torque constant (Nm/A), L_a is motor armature inductance (henry), R_a is motor armature resistance (ohm), s is a complex variable, f_v is viscous friction, J is the moment of inertia (kgm^2), K_b is back emf constant (Vs/rad), K is gain of position control, θ_o is angular position output, θ_i is angular position reference, K_T is constant, where $K_T = K_t / (R_af_v + K_tK_b)$, and τ is time constant, where $\tau = R_aJ / (R_af_v + K_tK_b)$.

Upon the receipt of the input signal, rotation was initiated by the motor, resulting in a corresponding adjustment of the cross-sectional area of the butterfly valve. This alteration subsequently impacted the mass flow rate of the recirculating air. Such a system can be considered by flowing through pipes with different cross-sectional areas as shown in Fig. 6.

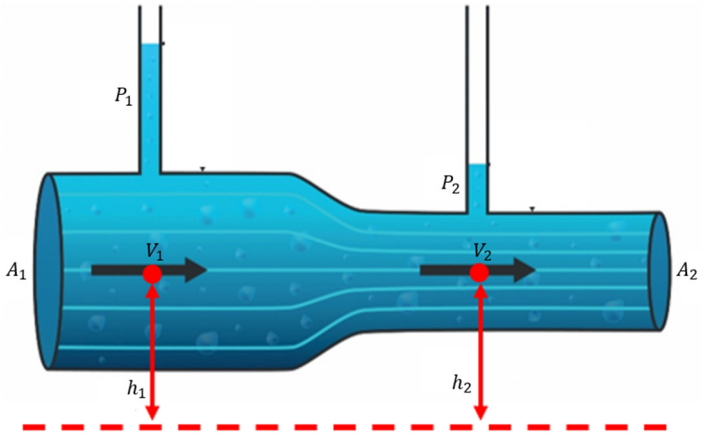

Fig. 6 Fluid flow through a pipe with different cross-sectional areas

The fluid flow from cross-sectional areas (A_1 to A_2) was described by the Bernoulli equation. When the fluid was incompressible and kept at the same height ($h_1 = h_2$), the fluid velocity at the exit could be estimated [25].

$$v_2(t)=\sqrt{\frac{2(P_1-P_2)}{\rho}+v_1^2} \tag{7}$$

To determine the mass flow change as the fluid flows through the control valve and solve this problem, the continuity equation and the Laplace transform were applied. The mass flow rate of the recirculating air through the control valve could be calculated as:

$$Q(s) = \rho(s) A(s) V_2(s) \tag{8}$$

When it is defined, $A(s) = K_1\theta(s)$ is the relationship between the linear cross-sectional area ($A(s)$) and the gate position of the valve ($\theta(s)$), and K_1 is the constant of proportionality. Therefore, the transfer function of the drying air flow rate was changed by the rotation of the control valve (G_{valve}) shown as:

$$G_{valve}(s) = \frac{Q(s)}{\theta(s)} = \rho(s) V_2(s) K_1 \tag{9}$$

When considering that air mixing was a time-independent value x(t), the Laplace transform of the function was represented by,

$$G_{mixing\ point}(s) = \frac{\omega_3(s)}{Q(s)} = X(s) \tag{10}$$

where v_1 is velocity of the fluid at point 1 (m/s), v_2 or V_2 is the velocity of fluid at point 2 (m/s), ρ is fluid density (kg/m^3), P_1-P_2 is pressure difference (Pa), Q is the mass flow rate at point 2 (kg/s), K_1 is the constant of proportionality, X is the proportion of the air mixing process, and ω_3 is the humidity ratio of mixed air (g_w/kg_{da}).

The total transfer function of the system (G_{total}) according to Fig. 4 was obtained by combining the blocks from the 3 main parts reported previously, as shown in the formula.

$$G_{total}(s) = \frac{\omega_3(s)}{\theta_t(s)} = \frac{K_T K K_1 \rho(s) V_2(s) X(s)}{\tau s^2 + s + K_T} \tag{11}$$

2.4. *Identification of the humidity control system from recirculating drying air*

System identification is a mathematical modeling method for dynamic systems. It uses experimental input and system response data in modeling [26-27]. This research used closed-loop experimental data collection in the time domain for system identification with MATLAB program. The least-squares method was compared to the general model of the second-order system described in Section 2.3. The sequence of steps to system identification can be schematically represented in Fig. 7.

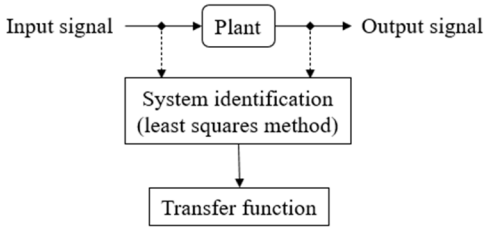

Fig. 7 System identification procedure

2.5. *Proportional Integral (PI) controller design*

The design of the system controller starts from setting the design specifications. Steady-state errors (E_{ss}) are zero, percent overshoot ($\%OS$) is less than 25%, and settling time at 2% error (T_s) is less than 60 seconds. These requirements are used to calculate the design point according to [28].

$$\zeta = \sqrt{\frac{\ln^2(\%OS)}{\ln^2(\%OS) + \pi^2}} \tag{12}$$

$$\omega_n = \frac{4}{T_s \zeta} \tag{13}$$

$$S_{1,2} = -\zeta\omega_n \pm j\omega_n\sqrt{1-\zeta^2} \tag{14}$$

Then, the root locus was analyzed to determine the proportional gain and integral gain under the angle condition and the magnitude condition. The PI controller was in the form of a transfer function according to [28].

$$G_{PI} = K_P + \frac{K_I}{s} = \frac{K_P(s+Z_c)}{s} \tag{15}$$

where ζ is the damping ratio, ω_n is the natural frequency, $S_{1,2}$ is the dominant pole for a design point, G_{PI} is the transfer function of the PI controller, K_P or K_I is controller gain, and Z_c is zero.

The feedback control system for controlling humidity ratio in the air circulation system is shown in Fig. 8, where the block diagram above (plant) was a command through the Arduino support package in the actual system operation, and the block diagram below was a mathematical model derived from system identification. The output signals from both sources were compared to the setpoint value.

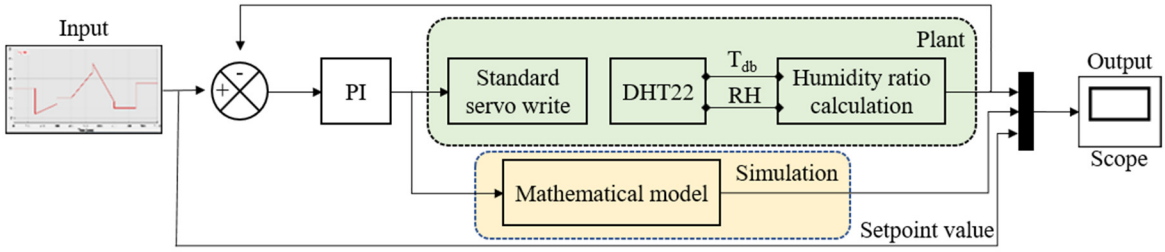

Fig. 8 Schematic diagram of a closed-loop humidity ratio control system

3. Result and Discussion

In this section, the results of the drying air recirculation test are discussed. To control the system and evaluate the performance of the controller, the transfer function obtained through system identification techniques was deployed.

3.1. The ability of the valve to adjust drying air circulation

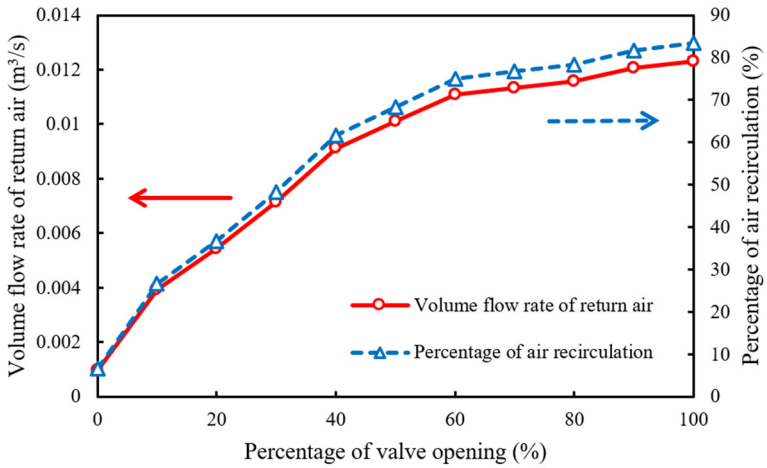

Fig. 9 The relationship between the input signal and the air recirculation

The response of the butterfly valve was evaluated with various input signals, as shown in Fig. 9. Results indicate that the volumetric flow of return air increased proportionally to the input signal in the range from 0% (valve at angle 0 degrees, air return leak of 0.0009 m^3/s) to 50% (valve at angle 45 degrees, air return of 0.01 m^3/s). Air circulation is reused up to 68.33%

when compared to the use of unmixed drying air in a drying chamber. However, this experiment limits the volumetric flow of drying air in the range of 60% (valve open at an angle of 54 degrees) onwards, and the system has the potential to 83% air recirculation when the valve is fully open.

3.2. System identification result of the humidity ratio control system

From the system identification according to Section 2.4, it was found that the least-squares method can estimate the variables present in the second-order transfer function as:

$$G_{total}(s) = \frac{0.002263}{s^2 + 0.2842s + 0.01332} \tag{16}$$

The estimation results correspond to the experimental data as 85.51%, and the root mean square error (RMSE) stands at 0.288. Considering the accuracy of this model and the research of Pongam et al. [29], which identified the thermal system identity of the reheating furnace for the design of the PI controller similarly, it was seen that this model was accurate enough to be used to design a controller and simulate the system response before being applied to control the actual system.

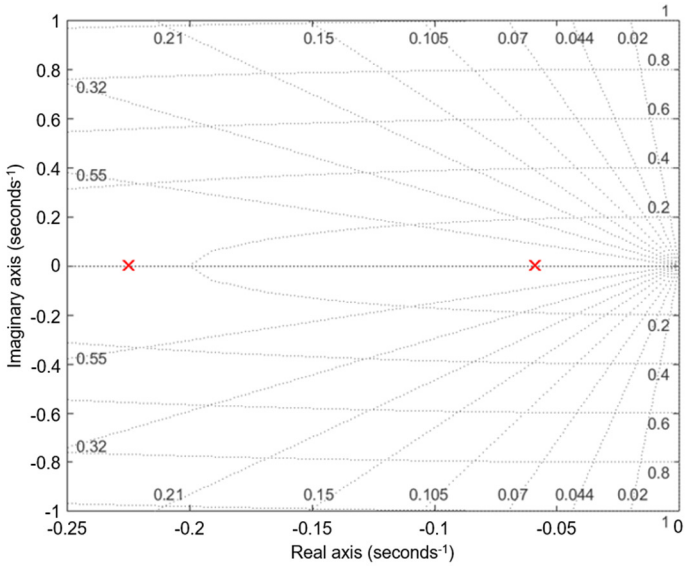

Fig. 10 Pole-Zero map of the system

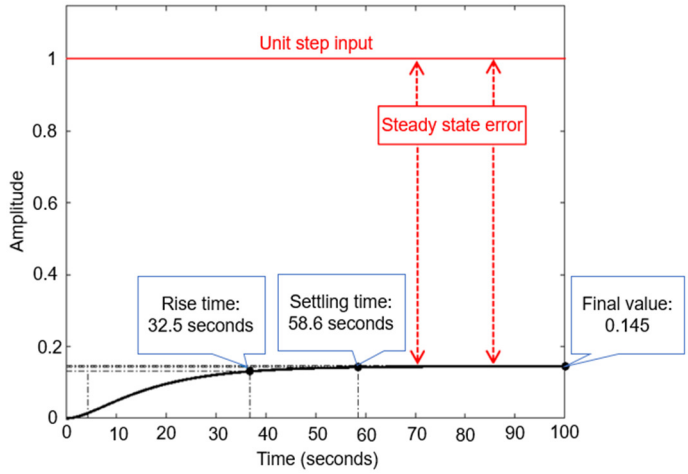

Fig. 11 The response to the unit step function of the system

From considering the closed-loop system of Eq. 10, it was found that the system has 2 poles, -0.0742 and -0.21, located on the real number axis as shown in Fig. 10. When testing the transfer function with a unit step input, it was found that the transient response in terms of the rise time was 32.5 seconds, the settling time at 2% error was 58.6 seconds, and response in

steady state was 0.145 (Setpoint = 1 in unit step input), which appears to have an offset error as in Fig. 11 due to the type 0 of open-loop transfer function. Therefore, it is necessary to minimize steady state error with the PI controller according to Section 2.5.

3.3. Proportional integral (PI) controller

Fig. 12 shows the pole and zero map of the system that was compensated by the PI controller. The proportional gain was 11.22, and the integral gain was 0.9884, which resulted in the system behaving according to the design conditions outlined in Eq. 14. The presence of complex conjugate poles on plane -0.0837 ± *j* 0.11 led to an oscillating effect on the unit step function, as shown in mathematical simulation (Fig. 13). The system had an overshoot of 16.5% (less than 25%) and settling time (2% of error) of 42.8 (less than 60 sec), which was following the established design conditions as shown in Table 1. Therefore, these gain values were tested with the air humidity ratio control system after the recirculation drying air mixing process. Fig. 14 shows the system response to PI controller operation. The process value was the air humidity ratio from the actual experiment, and the simulation was the response from the mathematical model compensated by a PI controller.

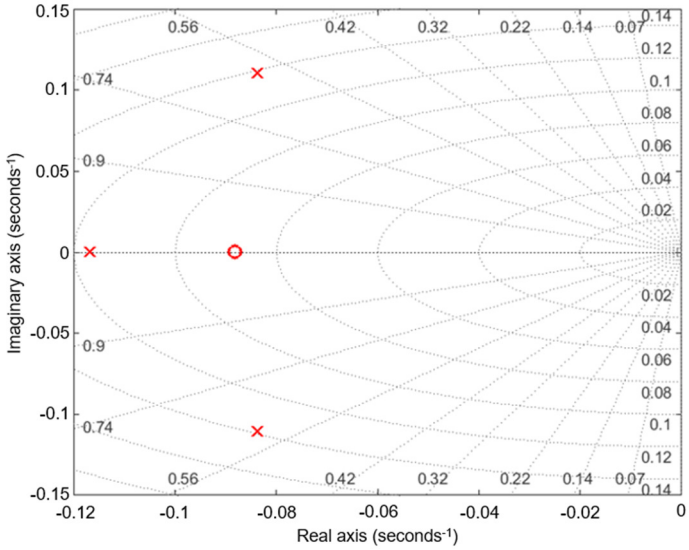

Fig. 12 Pole-Zero map of the system compensated by PI controller

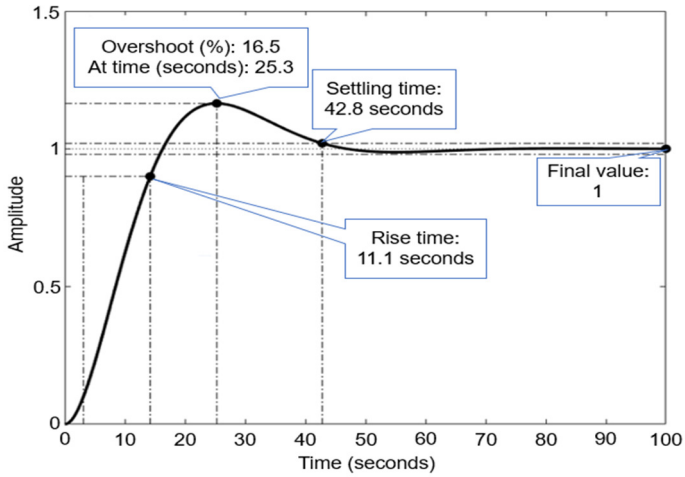

Fig. 13 Simulation of the unit step response of system compensated by PI controller

Table 1 The unit step response of the system: before and after compensation by the controller

System	Rise time (s)	Overshoot (%)	Settling time (s)	Final value
Requirements	-	Less than 25%	60	-
Before compensation	32.5	-	58.6	0.145
After compensation	11.1	16.5	42.8	1

The accuracy of describing the data from the mathematical model with system identification was as high as 85.51%, resulting in a corresponding trend of the response between the mathematical model and the actual process value as shown in Fig. 14. Despite some discrepancies that resulted from both mechanical and thermal losses in the air mixing process, further study was necessary to assess the impact of these losses. However, the overall system could be seen to have effectively maintained the process response within acceptable limits, with a maximum percent overshoot of 25%, settling time at 52 seconds before reaching the setpoint value, which found a percent overshoot of less than 15% and settling time less than 20 seconds at every subsequent setpoint. The integral term from the controller has great potential to improve the E_{ss} value. This control system can track the setpoint and compensate for discrepancies, causing E_{ss} to eventually reach 0.

When comparing the system performance with the study conducted by Pakdeekaew et al. [20], it was observed that the humidity control system described in the reference study exhibited a faster response to the reference value, approximately 40% faster than the system implemented in this research. Nonetheless, this influence was prominent during the initial phase of the operation. In the next setpoint, it was found that the humidity control system of this research was able to respond to the dependent variable faster from the start, which was only 7% behind the reference study. The results of the response comparison are shown in Fig. 15 and Table 2. While the humidity control system in this study exhibited a slightly delayed response compared to the reference study, it is worth noting that the humidity control system described in the reference study had a limitation on the amount of air recirculation, which should not exceed 15.18% of the drying air used in the system. This limitation highlights the advantage of the humidity control system implemented in this research, particularly when there is a need for large quantities of recirculating drying air.

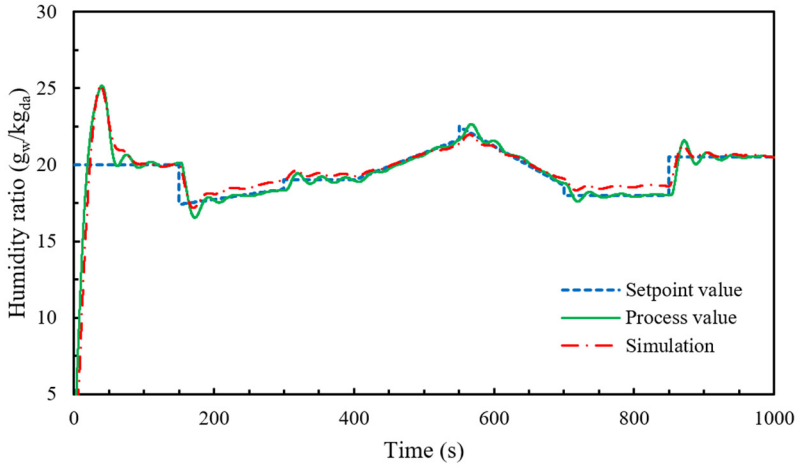

Fig. 14 System response from PI controller compensation

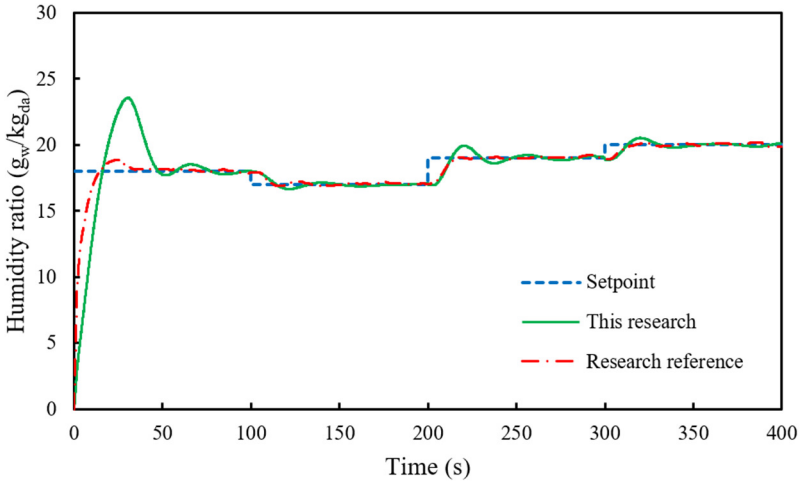

Fig. 15 Responses of the humidity control system at the same input

This system can recycle up to 83% of the drying air (Fig. 9), combined with the advantages of electric heating for the hot air system mentioned in the introduction. Therefore, the researcher has a guideline to apply this device for controlling the humidity and temperature in the paddy drying system. It is hoped that a highly precise control system that operates according to the optimal conditions plays a role in the energy efficiency of the drying process. It can reduce carbon emissions into the atmosphere compared to hot air combustion systems and being able to improve the quality of the product after drying in the future.

Table 2 The comparison between responses implemented in this research and the research reference

Setpoint (humidity ratio)	System	Overshoot (%)	Settling time (s)
18 g_w/kg_{da}	Research reference	4.22	32.70
	This research	23.65	45.68
17 g_w/kg_{da}	Research reference	0.71	109.44
	This research	2.07	110.80
19 g_w/kg_{da}	Research reference	0	212.39
	This research	4.76	227.25
20 g_w/kg_{da}	Research reference	0.15	309.45
	This research	2.60	324.30

4. Conclusions

This study developed an air recirculation system utilizing a servo motor to control a butterfly valve, thereby achieving proportional recirculation of dry air to mix with the intake air. An air circulation test observed a consistent and proportional increase in the volumetric flow of return air increased proportionally quite constant during the input signal. The defined input signal, represented by the percentage of valve opening, corresponded to the humidity ratio of the air obtained from the mix of return air and ambient air. Employing the system identification method, the mathematical model of the system was analyzed. The research defined specific design conditions to ensure zero steady-state error, a percentage overshoot of less than 25%, and a settling time was within 60 seconds. Through systematic system simulations utilizing a unit step function, it was determined that the proportional gain of 11.22 and the integral gain of 0.9884 fulfilled the design requirements, resulting in a percentage overshoot of 16.5% and a settling time of 42.8 seconds. Subsequent testing of the designed PI controller was tested against the actual air humidity ratio control system and revealed that the controller had sufficient potential to compensate for the system. In the future, it has the potential to further expand this system to control the air conditions on the industrial scale of drying systems.

Conflicts of Interest

The authors declare no conflict of interest.

References

[1] N. K. Fukagawa and L. H. Ziska, “Rice: Importance for Global Nutrition,” Journal of Nutritional Science and Vitaminology, vol. 65, no. Supplement, pp. S2-S3, 2019.
[2] S. Roman, L. M. Sánchez-Siles, and M. Siegrist, “The Importance of Food Naturalness for Consumers: Results of a Systematic Review,” Trends in Food Science & Technology, vol. 67, pp. 44-57, September 2017.
[3] D. Kumar and P. Kalita, “Reducing Postharvest Losses during Storage of Grain Crops to Strengthen Food Security in Developing Countries,” Foods, vol. 6, no. 1, article no. 8, January 2017.
[4] A. Müller, M. T. Nunes, V. Maldaner, P. C. Coradi, R. S. de Moraes, S. Martens, et al., “Rice Drying, Storage and Processing: Effects of Post-Harvest Operations on Grain Quality,” Rice Science, vol. 29, no. 1, pp. 16-30, January 2022.
[5] R. O. Lamidi, L. Jiang, P. B. Pathare, Y. D. Wang, and A. P. Roskilly, “Recent Advances in Sustainable Drying of Agricultural Produce: A Review,” Applied Energy, vol. 233-234, pp. 367-385, January 2019.
[6] M. Aghbashlo, H. Mobli, S. Rafiee, and A. Madadlou, “A Review on Exergy Analysis of Drying Processes and Systems,” Renewable and Sustainable Energy Reviews, vol. 22, pp. 1-22, June 2013.

[7] R. Indiarto, A. H. Asyifaa, F. C. A. Adiningsih, G. A. Aulia, and S. R. Achmad, "Conventional and Advanced Food-Drying Technology: A Current Review," International Journal of Scientific & Technology Research, vol. 10, no. 1, pp. 99-107, January 2021.
[8] W. Jittanit, N. Saeteaw, and A. Charoenchaisri, "Industrial Paddy Drying and Energy Saving Options," Journal of Stored Products Research, vol. 46, no. 4, pp. 209-213, October 2010.
[9] M. H. T. Mondal, K. S. P. Shiplu, K. P. Sen, J. Roy, and M. S. H. Sarker, "Performance Evaluation of Small Scale Energy Efficient Mixed Flow Dryer for Drying of High Moisture Paddy," Drying Technology, vol. 37, no. 12, pp. 1541-1550, 2019.
[10] M. Yapha, P. Bunyawanichakul, and N. Hayinilah, "Must Flow Dryer for Rough Rice," The Second International Conference on Green Computing, Technology and Innovation, the Asia Pacific University of Technology and Innovation, pp. 26-30, March 2014.
[11] P. Thauynak, M. Chuchonak, M. Yapha, and P. Bunyawanichakul, "Influences of Flow Velocity of Hot Air to Moisture Content Reduction of Paddy in Must Flow Paddy Dryer," Srinakharinwirot Engineering Journal, vol. 9, no. 1, pp. 28-35, July 2014. (In Thai)
[12] J. Havlík, T. Dlouhý, and M. Sabatini, "The Effect of the Filling Ratio on the Operating Characteristics of an Indirect Drum Dryer," Acta Polytechnica, vol. 60, no. 1, pp. 49-55, March 2020.
[13] S. Firouzi, M. R. Alizadeh, and D. Haghtalab, "Energy Consumption and Rice Milling Quality Upon Drying Paddy with a Newly-Designed Horizontal Rotary Dryer," Energy, vol. 119, pp. 629-636, January 2017.
[14] Ministry of Energy (Thailand), "20-Year Energy Efficiency Development Plan (2011-2030)," https://www.eppo.go.th/images/POLICY/ENG/EEDP_Eng.pdf, January 23, 2023.
[15] R. P. Amantéa, M. Fortes, and G. T. Santos, "Exergy Analysis Applied to the Design of Grain Dryers with Air Flow Recirculation," 2012 Dallas, Texas, July 29-August 1, 2012. American Society of Agricultural and Biological Engineers, article no. 121340983, 2012.
[16] B. Sila, A. Pakdeekaew, K. Treeamnak, and T. Treeamnak, "Effect of Exhaust Air Recirculation on Energy Consumption in Air Heating System," Proceeding of 14th Conference of Electrical Engineering Network 2022, May 2022. (In Thai)
[17] H. Darvishi, M. Azadbakht, and B. Noralahi, "Experimental Performance of Mushroom Fluidized-Bed Drying: Effect of Osmotic Pretreatment and Air Recirculation," Renewable Energy, vol. 120, pp. 201-208, May 2018.
[18] R. A. Chayjan, A. Ghasemi, and M. Sadeghi, "Stress Fissuring and Process Duration during Rough Rice Convective Drying Affected by Continuous and Stepwise Changes in Air Temperature," Drying Technology, vol. 37, no. 2, pp. 198-207, 2019.
[19] M. Tohidi, M. Sadeghi, and M. Torki-Harchegani, "Energy and Quality Aspects for Fixed Deep Bed Drying of Paddy," Renewable and Sustainable Energy Reviews, vol. 70, pp. 519-528, April 2017.
[20] A. Pakdeekaew, K. Treeamnuk, T. Treeamnuk, and N. Wongbubpa, "Application of Pulse Width Modulation Technique in Air Humidity Control System," Agriculture and Natural Resources, vol. 57, no. 2, pp. 321-330, March-April 2023.
[21] I. Golpour, R. P. Guiné, S. Poncet, H. Golpour, R. Amiri Chayjan, and J. Amiri Parian, "Evaluating the Heat and Mass Transfer Effective Coefficients during the Convective Drying Process of Paddy (Oryza sativa L.)," Journal of Food Process Engineering, vol. 44, no. 9, article no. e13771, September 2021.
[22] 2009 ASHRAE Handbook: Fundamentals, SI ed., Atlanta GA: American Society of Heating Refrigeration and Air-Conditioning Engineers, 2009
[23] L. A. Aloo, P. K. Kihato, and S. I. Kamau, "DC Servomotor-Based Antenna Positioning Control System Design Using Hybrid PID-LQR Controller," European International Journal of Science and Technology, vol. 5, no. 2, pp. 17-31, March 2016.
[24] A. Rajasekhar, P. Kunathi, A. Abraham, and M. Pant, "Fractinal Order Speed Control of DC Motor Using Levy Mutated Artificial Bee Colony Algorithm," 2011 World Congress on Information and Communication Technologies, pp. 7-13, December 2011.
[25] R. W. Fox, A. T. McDonald, P. J. Pritchard, and J. W. Mitchell, Fluid Mechanics, London: Wiley Global Education, 2016.
[26] M. Rajalakshmi, V. Saravanan, V. Arunprasad, C. A. T. Romero, O. I. Khalaf, and C. Karthik, "Machine Learning for Modeling and Control of Industrial Clarifier Process," Intelligent Automation & Soft Computing, vol. 32, no. 1, 2022.
[27] L. Ljung, "Perspectives on System Identification," Annual Reviews in Control, vol. 34, no. 1, pp. 1-12, April 2010.
[28] K. Ogata, Modern Control Engineering, 5th ed., Boston: Prentice-Hall, 2010.
[29] T. Pongam, J. Srisertpol, and V. Khompis, "PI Controller Design for Temperature Control of Reheating Furnace Walking Hearth Type in Setting Up Process," Advanced Materials Research, vol. 748, pp. 801-806, August 2013.